Optimization of Polymer Synthesis Through Distributed Control of Polymerization Conditions

AVIEL FALIKS,[1] RICHARD A. YETTER,[2]* CHRISTODOULOS A. FLOUDAS,[3] YEN WEI,[4] HERSCHEL RABITZ[1]

[1] Department of Chemistry, Princeton University, Princeton, New Jersey

[2] Department of Mechanical and Aerospace Engineering, Princeton University, Princeton, New Jersey

[3] Department of Chemical Engineering, Princeton University, Princeton, New Jersey

[4] Department of Chemistry, Drexel University, Philadelphia, Pennsylvania

Received 12 June 2001; accepted 27 November 2001

ABSTRACT: An optimal control methodology is applied to the goal of lowering polydispersity while increasing conversion in polymerization reactions. An illustration using initiator, heat, and monomer flux control profiles for free-radical polymerization of styrene in a plug flow reactor is provided and compared with available experimental data. The design calculations use a kinetic model that includes the gel effect. The reactor designs show that distributed initiator, heat, and monomer fluxes along the length of the reactor lower the polydispersity of the styrene polymers and increase conversion for a given reaction time. The monomer flux maintains a nearly constant monomer concentration in the reactor. The initiator and heat fluxes are highly correlated. The temperature rises as a result the heat flux; but the initiator flux results in a lower initiator concentration relative to the initiator cofeed case. At a reaction time of 120 min, a conversion of 44% and a polydispersity of 1.73 have been achieved. The theoretical designs, although not proven to be globally optimal, are of high quality.
 J Appl Polym Sci 85: 2922–2928, 2002

Key words: distributed control polymerization; plug flow reactor; free-radical polymerization; polystyrene; theoretical modeling

INTRODUCTION

Polymer syntheses are carried out by a remarkable variety of processes. Most high-performance polymers, and almost all high-value polymer are made by batch processes. One reason is that a long reaction time may be required to convert monomer to polymer. To allow such residence times in continuous reactors, a very large capacity or long units would be required, at enormous capital expense. For this reason, significant work has been done to optimize polymerization processes so that they may be done in a continuous fashion.[1–4] None of the these efforts have attempted to optimize the distribution of energy and/or mass along the reactor length. As a consequence, the polymer yields from any particular reactor design represent a lower bound on what might be achieved. Thus, it is desirable to explore the improved polymer yields from an optimal design of distributed energy and input chemical flux along the length of the reactor.

Correspondence to: H. Rabitz (hrabitz@princeton.edu).
**Current address:* Department of Mechanical and Nuclear Engineering, Pennsylvania State University, University Park, PA 16802.

Journal of Applied Polymer Science, Vol. 85, 2922–2928 (2002)

The homogeneous free-radical polymerization of styrene has been used as a model reaction for studying polymer reactors,[1,2] as it is a well-understood process with accurate kinetic and thermodynamic data available.[1,2,5] In addition, Wallis et al.[4] showed that production of quality polystyrene for industrial purposes in a tubular reactor is feasible and reproducible. The aim of this article is to show that special designs of initiator, heat, and monomer fluxes along the length of a tubular plug flow reactor (PFR) may produce a polymer of a desired average molecular weight with as narrow a molecular weight distribution as possible while maintaining the highest possible conversion. Here, we apply a previously developed optimal control methodology for a PFR with variable heat and mass fluxes along the reactor's length. This methodology has been applied to complex reaction mechanisms, and high-quality solutions were obtained.[6] Whereas the reactor model used here is similar to the one in that paper, the chemical model has been replaced with a polymerization mechanism that incorporates the gel effect to account for the decrease in the termination rate caused by the increased viscosity that results from high conversion.

In this article, the reactor model is presented and an optimal control design is demonstrated to improve on a design that does not incorporate distributed control. The applicability of the process for laboratory implementation is also discussed. The optimal control formulation is presented in the Appendix.

MODELING

Physical Formulation of the Flow Reactor

A PFR was chosen as the basic reactor configuration. The PFR is a cylinder with constant cross-sectional area and length L. Control is implemented through chemical and/or heat flux through the side wall of the reactor as a function of the position l along its length. The reactions are described by the production rate w_i of the i-th species, $i = 1, 2, \ldots, n$. The control variables are the fluxes of species i, denoted as j_i (mass/length − time), and the heat flux, q (energy/length − time), as a function of position l. The mass fraction of species i in the reactor is denoted as $x_i(l)$, and the total mass flow rate is $F(l)$.

The following assumptions were made in modeling the PFR: (1) steady one-dimensional plug flow, (2) instantaneous radial mixing, (3) no diffusion along the axis of the reactor, and (4) adiabatic reaction conditions. To make the assumptions realistic, the ratio of the length of the reactor to its radius was chosen to be > 25.

As there are two sources of material flowing into the system (a cofeed and an axial mass flux), the total mass balance for the flow rate is given in eq. (1):

$$F(l) = F(0) + \int_0^l \sum_{i=1}^{n} j_i dl. \tag{1}$$

By taking a differential control volume at position l and balancing the input and output mass and energy, we can arrive at the equations governing the composition in the reactor. Considering the conservation of mass, the species balance equation is

$$Fx_i + j_i dl + w_i dl = \left(F + \frac{dF}{dl}\,dl\right)\left(x_i + \frac{dx_i}{dl}dl\right) = (F + \sum_{i=1}^{n} j_i dl)\left(x_i + \frac{dx_i}{dl}\,dl\right). \tag{2}$$

The first term on the left represents the amount of the i-th species flowing into the control volume. The second and third terms, respectively, represent the amount of the species influx added from the side of the reactor and the amount produced or consumed in chemical reactions within the volume. Taking the infinitesimal limits of dx_i and dl, we arrive at the mass conservation equation

$$\frac{dx_i}{dl} = \frac{1}{F}\,(w_i - x_i \sum_{k=1}^{n} j_k + j_i). \tag{3}$$

A similar approach may be used to derive the energy conservation equation

$$T\sum_{i=1}^{n} C_{p_i} F x_i + (T_0 \sum_{i=1}^{n} C_{p_i} j_i + q)dl - \sum_{i=1}^{n} H_{fi} w_i dl = (T + dT)\left[\sum_{i=1}^{n}\left(F + \frac{dF}{dl}dl\right)\left(x_i + \frac{dx_i}{dl}dl\right)C_{p_i}\right] = \left(T + \frac{dT}{dl}dl\right)\left[\sum_{i=1}^{n}(F + \sum_{i=1}^{n} j_i dl) \times \left\{x_i + \left(\frac{1}{F}(w_i - x_i \sum_{k=1}^{n} j_k + j_i)\right)dl\right\}C_{p_i}\right], \tag{4}$$

where q is the heat influx, H_{f_i} is the heat of formation of species i, and C_{p_i} is the corresponding specific heat. T_0 is the temperature of the influxed species. Taking the infinitesimal limits of dx_i and dl leads to the energy conservation equation

$$\frac{dT}{dl} = \frac{1}{F\sum_{i=1}^{n} C_{p_i} x_i} [(T_0 - T)\sum_{i=1}^{n} C_{p_i} j_i - \sum_{i=1}^{n} H_{f_i} w_i - T\sum_{i=1}^{n} C_{p_i} w_i + q]. \quad (5)$$

Polymerization Model

The polymerization mechanism[2,3,7–11] consisted of the following key steps:

$$\text{Initiation} \qquad I \xrightarrow{k_d} 2R_c; \quad (6)$$

$$R_c + M \xrightarrow{k_{p1}} R_i; \quad (7)$$

$$\text{Propagation} \qquad R_r + M \xrightarrow{k_p} R_{r+1}; \quad (8)$$

Chain Transfer

$$\text{to monomer} \qquad R_r + M \xrightarrow{k_{tm}} P_r + R_1; \quad (9)$$

$$\text{to solvent} \qquad R_r + S \xrightarrow{k_{ts}} P_r + S^*; \quad (10)$$

Termination

$$\text{combination} \qquad R_r + R_s \xrightarrow{k_{tc}} P_{r+s}; \quad (11)$$

$$\text{disproportionation} \qquad R_r + R_s \xrightarrow{k_{td}} P_r + P_s. \quad (12)$$

Here, I represents the initiator, M is the monomer (styrene), S is the solvent, R_r is a growing polymer of length r, and P_r is a dead polymer of length r. R_c is a radical that is formed from the initiator, and S^* is a radical fragment of the solvent. The rate constants used are given in Table I.[2,3,7,8]

Yamada et al.[7,10,11] have shown that the rate of propagation for polystyrene radicals remains constant over a polymerization range of $40 \leq R_r \leq 410$. In addition, they have also demonstrated that the propagation rate remains constant at higher conversion. Because of the increased viscosity that results from increases in the molecular weight of polymer chains, the termination rate does not remain constant but decreases, leading to the gel effect. The gel effect has been incorporated into the mechanism by considering the effective rate of termination, k_t as a function of monomer conversion, m:

$$k_t = k_{tc} + k_{td}, = A_t \exp[-E_a/RT]g^2(m), \quad (13)$$

where k_{tc} and k_{td} are the recombination and disproportionation termination constants, respectively, and

$$g(m) = \begin{cases} 1 & \text{as } 0 \leq m \leq m_1 \\ 0.5093 + 2.4645m - 3.7473m^2 & \text{as } m \geq m_1 \end{cases}, \quad (14)$$

where m_1 is the monomer conversion at which the gel effect is appreciable and is equal to 0.3 in our model.[8,12]

Thermodynamic data for heat capacity and heat of formation of styrene were taken from the work of Gaur and Wunderlich[5] by a fit of the data in Table 3 of their work. The initiator efficiency f, the probability factor for a primary radical to undergo reaction with a monomer, rather than combine with another radical and form a "dead" product,[3] is set equal to 0.6.

Table I Rate Parameters[a]

k_d	$= 1.58 \times 10^{15} \exp[-30800/RT] s^{-1}$
k_{p1}	$= 1.255 \times 10^9 \exp[-1680/RT]$
k_p	$= 1.051 \times 10^7 \exp[-7060/RT]$
k_{tm}	$= 2.31 \times 10^6 \exp[-12670/RT]$
k_{ts}	$= 5.92 \times 10^8 \exp[-17210/RT]$
k_{tc}	$= 9.98 \times 10^5$
k_{td}	$= 1.10 \times 10^7 \exp[-3750/RT]$

[a] Rate constant units not shown are L s^{-1} mol^{-1}. Activation energies are in calories.

COMPUTATIONAL STUDIES

The reactor design was applied to a reference case and a test problem where initiator, heat, and

monomer fluxes were optimized. In the optimization example, an effective strategy for finding a cost functional minimum involved making several calculations with increasingly demanding objectives. The optimal flux profiles of the previous simulation were found to be good initial points for subsequent calculations. The computer code employed for these simulations has performed well in previous applications.[6,13,14] It is important to note that this work serves to show the general significance of optimally controlling polymer synthesis rather than attempting to corroborate any specific reaction mechanism or experiment.

The average iteration took about 53 minutes of CPU time on an R4000 IRIS Indigo. Although global optimality could not be guaranteed, it is evident that good-quality solutions were obtained using the proposed algorithm. In the examples, the length of the PFR in which the polymerization takes place is $L = 100$ cm, with a cross-sectional area of 40 cm^2.

The results for the reference case are shown in Figure 1. The experimental data shown are from Blavier and Villermaux.[2] The initial monomer concentration is 6.65 mol L^{-1}. The initiator used is Azo-bis-isobutyronitrile (AIBN), and its initial concentration is 0.0333 mol L^{-1}. The solvent is cyclohexane with an initial concentration of 2.22 mol L^{-1}. The temperature is 348 K. Both conversion and polydispersity are in close agreement with the experimental data. After 120 minutes, the reference case shows a conversion of 37% and a polydispersity of 1.97.

Figure 2 shows the results for an optimized simulation. The initial concentrations of monomer and solvent are identical to the reference case. There is no cofeed of initiator, and the initial temperature is 346 K. The desired chain length is 200 units, and a penalty is used that increases away from the desired length. The distributed control of the initiator, heat, and monomer results in the conversion increasing to 44% and the polydispersity decreasing to 1.74 in comparison with the reference case. Such a decrease in the polydispersity is quite significant. It is noteworthy that most nonliving radical polymerizations give broad polydispersities, typically 2–5; with consideration of the gel effect, polydispersity can be as high as 5–10.[15]

The total amount of monomer fluxed into the reactor is 0.35 of the monomer cofeed. The extra flux serves to keep the monomer concentration roughly constant, thereby increasing conversion. In addition, the monomer flux reduces the chance

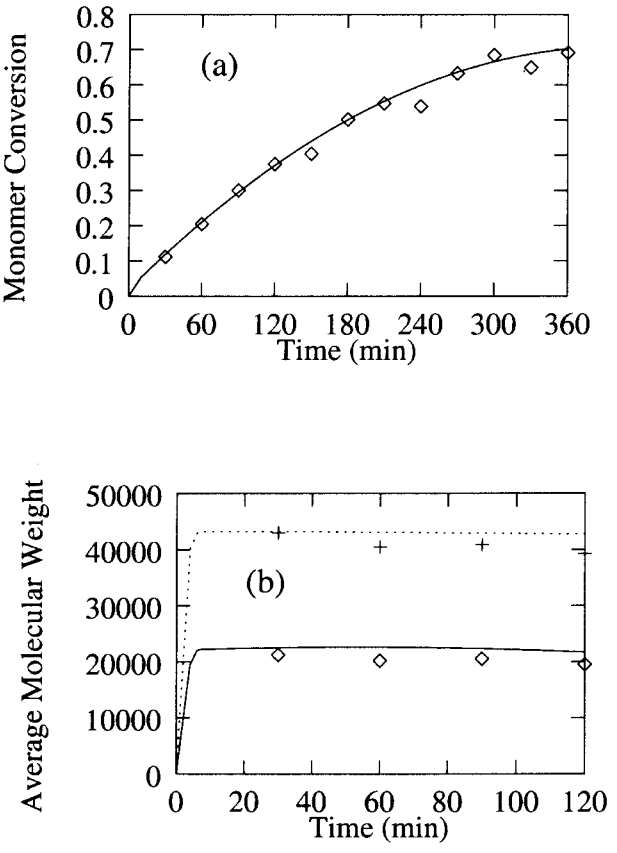

Figure 1 Results based on experimental conditions with no optimization: (a) monomer conversion as a function of time; and (b) M_n (solid line) and M_w (broken line) as a function of time. Solid lines are simulation results, points are experimental data. All experimental data are from Blavier and Villermaux.[2]

of two chains colliding and terminating, which lowers the polydispersity. The initiator and heat flux are closely correlated. Optimizations of the initiator and heat alone did not result in significant improvements for a given residence time and desired chain length. The use of a heat flux to raise the temperature, however, can lower the polydispersity for a given residence time and desired chain length if the initiator addition is optimized as well. The total initiator added to the reactor is then lowered to 0.53 of the initiator cofed in the reference case. The distributed nature of the initiator flux in the first part of the reactor, combined with the distributed monomer flux, keeps the initiator concentration roughly constant in the first part of the reactor and helps lower the polydispersity and increase the conversion.

The residence time of 120 minutes and chain length of 200 U have been chosen arbitrarily to

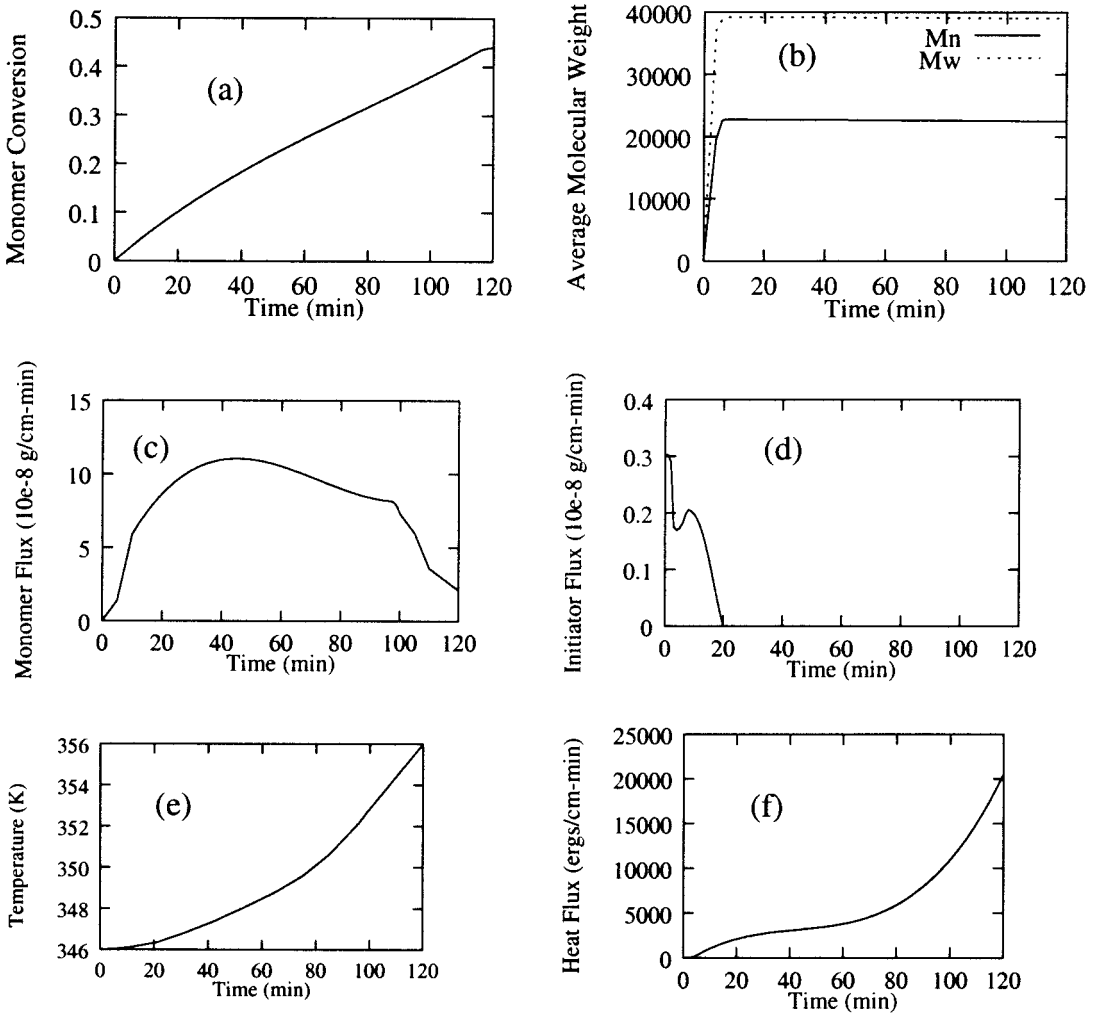

Figure 2 Results from optimization of initiator, monomer and heat: (a) monomer conversion as a function of time; (b) M_n and M_w as a function of time; (c) optimized monomer flux as a function of time; (d) optimized initiator flux as a function of time, (e) temperature profile; and (f) heat flux as a function of time.

demonstrate the principles of optimal control. Similar results may be obtained for other residence times and chain lengths. The resulting fluxes also have similar shapes to the fluxes presented in Figure 2.

CONCLUSIONS AND REMARKS

The optimal control of polymer synthesis in a PFR has been considered with an illustration for the free-radical polymerization of styrene. It was shown that optimally designed initiator, heat, and monomer fluxes along the length of the reactor can increase conversion and decrease polydispersity. As global optimality was not guaranteed, even better results may be achievable.

It is important to emphasize that the methodology employed in this work is general and may be used in various polymerization processes including catalyzed polymerizations and reactions that do not necessarily involve radicals. Optimal control will yield results that are at least as attractive as those achieved by conventional reactor design.

In the laboratory, the theoretical solutions presented in this article can serve as starting points for a reactor with feedback to refine the control design. The output performance of the reactor would be fed to a learning algorithm, to in turn

design the next experiment in a repeated sequence. This self-optimization is independent of the model assumptions that were used in the theoretical work and will therefore bring forth the most refined synthesis products.

APPENDIX

Optimal Control Formulation

The goal is to manipulate j and q, the input fluxes, so as to approach the optimal composition vector x while obeying conservation eq. (3) and (5). Satisfaction of dynamic constraints imposed by mass and energy conservation is assured by introducing Lagrange multipliers.

The objective function J (x_i, j_i, q, T) for the optimal control problem can be formulated in many ways, but it is desirable that J be a smooth and convex function that is bounded from below.[16] The chosen objective function was

$$J = C + \sum_{i=1}^{n} \int_0^L \lambda_i \left[\frac{1}{F}(w_i - x_i \sum_{k=1}^{k=n} j_k + j_i) - \frac{dx_i}{dl} \right] dl + \int_0^L \lambda T \left[\frac{1}{F \sum C_{p_i} x_i} \left((T_0 - T) \sum_{i=1}^{n} C_{p_i} j_i - \sum_{i=1}^{i=n} H_{fi} w_i - T \sum_{i=1}^{i=n} C_{p_i} w_i + q \right) - \frac{dT}{dl} \right] dl, \quad (15)$$

where

$$C = \frac{1}{2} ((x'(L) - x^f)^T W_f (x'(L) - x^f)) + \frac{1}{2} \int_0^L x^T W_x x dl + \frac{1}{2} \int_0^L j^T W_j j dl + \frac{1}{2} \int_0^L q W_q q dl. \quad (16)$$

L is the total length of the reactor. C consists of four terms. The first term controls the composition of the mixture at the end of the reactor. The desired final composition is x^f and W_f is a positive weight matrix. The next three terms respectively minimize the concentrations of undesired species, species fluxes, and heat flux along the reactor? W_x and W_j are penalty weight matrices, W_q is a scalar penalty weight. The weight matrices are positive-definite and chosen to be diagonal to avoid any correlation terms. The equations describing the reactor are incorporated into J through the Lagrange multipliers[14] λ_i and λ_T. Pontryagin's maximum principle[17] then allows us to find the sufficient conditions for optimality:

$$\frac{\delta J}{\delta j_i} = \frac{\delta J}{\delta q} = \frac{\delta J}{\delta x_i} = \frac{\delta J}{\delta \lambda_i} = \frac{\delta J}{\delta_T} = 0, \quad (17)$$

$$\lambda_i(L) = \frac{\partial J}{\partial x_i(L)}, \quad (18)$$

$$\lambda_T(L) = \frac{\partial J}{\partial T(L)}. \quad (19)$$

The adjoint equations for the Lagrange multipliers are:

$$\frac{d\lambda_i}{dl} = -W_{x_{ii}x_i} + \frac{1}{F} \left(- \sum_{k=1}^{n} \lambda_i \frac{dw_k}{dx_i} + \lambda_i \sum_{k=1}^{n} jk + \frac{\lambda_T}{\sum C_{p_i} x_i} \times \left(\sum_{k=1}^{n} H_{fk} \frac{dw_k}{dx_i} + T \sum_{k=1}^{n} C_{p_k} \frac{dw_k}{dx_i} \right) \right) - \frac{\lambda_T C_{p_i}}{F(\sum C_{p_i} x_i)^2} \times \left((T_0 - T) \sum_{i=1}^{n} C_{p_i} j_i - \sum_{i=1}^{n} H_{fi} w_i - T \sum_{i=1}^{n} C_{p_i} w_i + q \right); \quad (20)$$

$$\frac{d\lambda_T}{dl} = -\frac{1}{F} \sum_{i=1}^{n} \lambda_i \frac{dw_i}{dT} + \frac{\lambda_T}{F \sum C_{p_i} x_i'} \left(\sum_{i=1}^{n} \left(H_{fi} \frac{dw_i}{dT} + \frac{dH_{fi}}{dT} w_i \right) \right) + \sum_{i=1}^{n} C_{p_i} j_i + T \sum_{i=1}^{n} C_{p_i} \frac{dw_i}{dT} + \sum_{i=1}^{n} C_{p_i} w_i, \quad (21)$$

where $W_{x_{ii}}$ is the (i,i) element of W_x

The endpoint conditions of the adjoint equations are:

$$\lambda_i(L) = W_{fi}(x_i(L) - x^f); \quad (22)$$

$$\lambda_T(L) = 0, \quad (23)$$

where W_{f_i} is the (i, i) entry in the W_f matrix.

The gradient of the objective function, which will be set equal to zero, can now be calculated as

$$\frac{\delta J}{\delta j_i} = w_{j_{ii}j_i} + \frac{\lambda_i}{F} - \frac{1}{F}\sum_{i=1}^{i=n}\lambda_i x_i - \int_1^L \frac{I}{F^2}\left(\sum_{i=1}^{i=n}\lambda_i\left(w_i - x_i\sum_{i=1}^{i=n} j_i + j_i\right) + \frac{\lambda_T}{\sum C_{p_i}x_i}\left((T_0 - T)\sum_{i=1}^{i=n}C_{p_i}j_i - \sum_{i=1}^{i=n} H_{f_i}w_i - T\sum_{i=1}^{i=n} C_{p_i}w_i + q\right)\right)dl + \frac{\lambda_T}{F\sum C_{p_i}x_i}C_{p_i}(T_0 - T); \quad (24)$$

$$\frac{\delta J}{\delta q} = w_q q + \frac{\lambda_T}{F\sum C_{p_i}x_i}, \quad (25)$$

where $W_{j_{ii}}$ is the (i, i) element of W_j.

In the calculations, the CONMIN[18] code was used as the conjugate gradient minimizer; the chemical kinetics package CHEMKIN-II[19] was employed to interface the thermodynamics and kinetics data, and LSODA[20] was used as a differential equation integrator.

To ensure positive mass flux densities j_i, a transformation to a new control variable j_i' was done where $j_i = \exp(j_i')$. The gradient is then modified to

$$\frac{\delta J(l)}{\delta j_i'(l)} = \exp(j_i')\frac{\delta J}{\delta j_i'(l)}. \quad (26)$$

We acknowledge support from the National Science Foundation. YW wishes to thank Drexel University for granting him a sabbatical leave at Princeton University.

REFERENCES

1. Chaimberg, M.; Cohen, Y. Ind Eng Chem Res 1990, 29, 1152.
2. Blavier, L.; Villermaux, J. Chem Eng Sci 1984, 39, 101.
3. Chen, S.; Jeng, W. Chem Eng Sci 1978, 33, 735.
4. Wallis, J.; Ritter, R.; Andre, H. AIChE 1975, 21, 686.
5. Gauer, U.; Wunderlich, B. J Phys Chem Ref Data 1982, 11, 313.
6. Rojnuckarin, A.; Floudas, C. A.; Rabitz, H.; Yetter, R. J Phys Chem 1993, 97, 11689.
7. Yamada, B.; Kageoka, M.; Otsu, T. Poly Bull 1992, 28, 75.
8. Chen, S.; Lin, K. Chem Eng Sci 1980, 35, 2325.
9. Moad, G.; Solomon, D. H.; Johns, S. R.; Willing, R. I. Macromolecules 1984, 17, 1094.
10. Yamada, B.; Kageoka, M.; Otsu, T. Polym Bull 1992, 29, 385.
11. Yamada, B.; Kageoka, M.; Otsu, T. Macromolecules 1991, 24, 5234.
12. Chen, S.; Huang, N. W. Chem Eng Sci 1981, 36, 1295.
13. Rojnuckarin, A.; Floudas, C. A.; Rabitz, H.; Yetter, R. Ind Eng Chem Res 1996, 35, 683.
14. Faliks, A.; Yetter, R. A.; Floudas, C. A.; Hall, R.; Rabitz, H. J Phys Chem A 2000, 104, 10740.
15. Odian, G. In Principles of Polymerization, 3rd ed.; Wiley; New York, 1991; pp 293–296.
16. Leigh, J. R. Functional Analysis and Control Theory; Academic Press: New York, 1980.
17. Bryson, A. E.; Ho, Y. Applied Optimal Control; Blaisdell: New York, 1973.
18. Shanno, D. F.; Phua, K. H. ACM Trans Mathematical Software 1980, 6, 618.
19. Kee, R. J.; Rupley, F. M.; Miller, J. A. CHEMKIN-II A Fortran Chemical Kinetics Package; Sandia National Laboratories, 1989.
20. Hindmarsh, A. C. Odepack, A Systemized Collection of Ode Solvers in Scientific Computing; North-Holland, 1983.